NJC

Accepted Manuscript

This is an *Accepted Manuscript*, which has been through the Royal Society of Chemistry peer review process and has been accepted for publication.

Accepted Manuscripts are published online shortly after acceptance, before technical editing, formatting and proof reading. Using this free service, authors can make their results available to the community, in citable form, before we publish the edited article. We will replace this *Accepted Manuscript* with the edited and formatted *Advance Article* as soon as it is available.

You can find more information about *Accepted Manuscripts* in the Information for Authors.

Please note that technical editing may introduce minor changes to the text and/or graphics, which may alter content. The journal's standard Terms & Conditions and the Ethical guidelines still apply. In no event shall the Royal Society of Chemistry be held responsible for any errors or omissions in this *Accepted Manuscript* or any consequences arising from the use of any information it contains.

ROYAL SOCIETY OF CHEMISTRY

www.rsc.org/njc

Nitric oxide inhibition, antioxidant and antitumour activities of novel copper(II) *bis*-benzimidazole diamide nano coordination complexes

Manisha Singla[a], Rajeev Ranjan[b], Kuldeep Mahiya[c], Subash C. Mohapatra[d*], Sharif Ahmad[e#]

[a,c]*Department of Chemistry, University of Delhi, New Delhi, India*

[b]*Department of Zoology, University of Delhi, New Delhi, India*

[d *]*Department of Chemistry, Atma Ram Sanatan Dharma College, University of Delhi, New Delhi, India*

[e#]*Department of chemistry, Jamia Millia Islamia, New Delhi, India*.

Corresponding Author: Dr. Subash C. Mohapatra[*]

E-mail **:** subashcm@gmail.com

Phone No. +91 11 24113436, ext. 3268; Fax No. +91 11 24111390

Abstract

Novel copper(II) nano coordination complexes [LCuCl]Cl **C1**, **[**LCu(SCN)]SCN **C2**, and [LCu(NO_3)]NO_3 **C3** capped by *bis*-benzimidazole diamide ligand N^1,N^5-*bis*{(1*H*-benzo[d]imidazole-2-yl)methyl}glutaramide L, have been synthesized and characterized by spectroscopic methods *viz* Transmission Electron Microscopy (5-100 nm), Dynamic Light Scattering, Elemental Analysis, EPR and Infrared Spectroscopy. These complexes also observed for inhibition of nitric oxide released significantly in culture. The Lipopolysaccharide induced super oxide production also decreased being most significant in complex **C2**. Nano coordination complex **C2** shows most significant *in vitro* cytotoxicity against human cervical cancer cell lines HeLa, MCF-7 and U-87 cells ranging from 50 μg/ml to 500 μg/ml. In *vivo* study revealed an increase in body weight (11.5 g) for tumour control groups, whereas in the case of mice groups treated with test sample **C3**, the difference in body weight was around 4.7 g. In further studies, it decreased to 2.2 g and 0.6 g in the case of mice groups treated with nano coordination complexes **C1** and **C2** respectively. The mean mice survival time was 21 days, which increased to 100, 120, and 170 days for **C3**, **C1**, and **C2**, respectively.

Keywords: Copper(II) nano coordination complexes, nitric oxide, antioxidant activity, antitumour activity, EPR, energy optimization.

1. Introduction

Development of modern technologies allows us to solve many therapeutic, medical and vetting problems. The development of new materials for effective drug delivery systems, diagnostics and control over patient treatment use nano coordination complexes for new medicines, biological applications and preparations. Many natural biological sites, such as the active centres of several metalloenzymes, are mostly due to transition metal ions; thus, synthetic mononuclear and binuclear receptors can be used to mimic the active centres,[1-4] which might be helpful for the healthy organisms. In healthy organisms, production of reactive oxygen species (ROS) and reactive nitrogen species (RNS) is approximately balanced by antioxidant defence systems and is related to 'oxidative stress'[5]. Recent studies have shown that RNS's, such as nitric oxide (NO), peroxynitrite ($ONOO^-$) and nitrogen dioxide (NO_2) also play an

important role in inflammatory processes[6,7] and carcinogenesis.[8] Thus it is very important to keep ROS and RNS at normal levels otherwise they can play a major role in mutations which cause DNA damage.[9-11]

Metal complexes have been extensively used as potential antitumour agents *viz.* the use of *cis*-platin in cancer chemotherapy,[12] while mixed ligand complexes play a key role in variety of biological systems.[13] These inventions lead us to the specific structural shapes of drug like entities,[13,14] which have been implicated in the storage and transport of active substances through membranes. Among these ligands, benzimidazole containing metal complexes and its derivatives are progressively used in bioinorganic systems[15], while the monomer copper(II) benzimidazole complexes exhibit a broad spectrum of biological activities.[16,17] Since, the benzimidazole moiety is a structural isostere of naturally occurring nucleotides; hence it has been extensively utilized as a drug scaffold in the medicinal value. Compounds containing benzimidazole nucleus have a wide spectrum of biological activity *i.e*. antifungal,[18, 19] antibacterial,[20,21] antimicrobial,[22,23] antiamobeic,[24,25] antiparasitic[26] and antitumour.[27,28] Recently, scientists have reported that benzimidazole analogues can be suitably modified by the introduction of different heterocyclic moieties, which exhibit a broad spectrum of biological activities such as potent anticancer and antifungal activity.[29,30] As we know, the benzimidazole derivatives serve as good ligands for transition metal ions due to the large conjugated π-systems and the imine nitrogen, which can affect positively the structures of the complexes.[31] The literature on different metal containing nano coordination complexes shows that their toxicity is 7-50 times less than the normal, due to their multifunctional and durable action, easy penetration into all organs and tissues, stimulation of metabolic processes when used in biotic doses.[32-34] With this idea, we are reporting the synthesis and characterization of novel benzimidazole containing copper(II) nano coordination complexes, having significant *in vivo* and *in vitro* antioxidant as well as antitumour activity. These complexes have also been observed for inhibiting NO release significantly in culture.

2. Results

2.1 Transmission electron microscopy (TEM) and dynamic light scattering (DLS)

TEM images show a nearly spherical distribution of the nano coordination complexes (Figure 1).

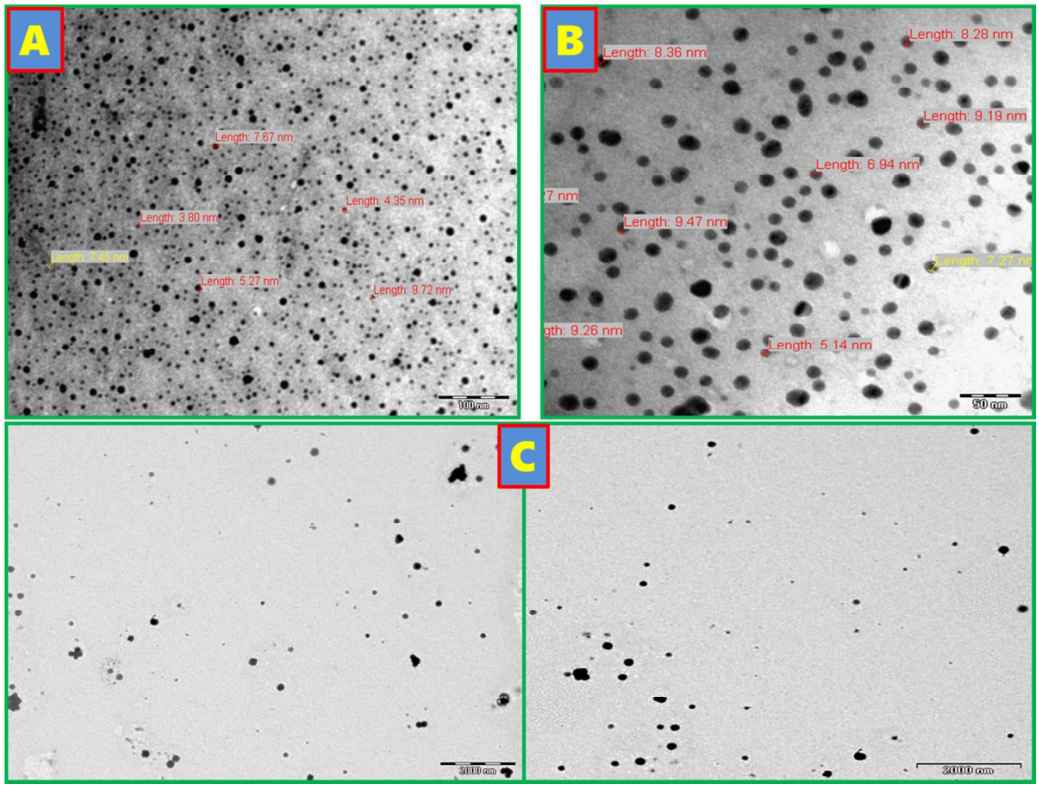

Figure 1. TEM micrograph of **C2** (A), **C1** (B) and **C3** (C) nano coordination complexes

The average size of the nano coordination complexes were obtained to be 5-10 nm for **C1** (with Cl^- as the co-anion) and **C2** (with SCN^- as the co-anion), while 80-100 nm for **C3** (with NO_3^- as the co-anion) (Table 1).

Cu(II) nano coordination complex	TEM (nm)	DLS (nm)[a] ± 1-3 nm Number of determinations/ cumulants (a) : 3	Width of hydrational sphere (nm)
[LCuCl]Cl (**C1**)	8	37	15
[LCuSCN]SCN (**C2**)	8	27	10
[LCu(NO_3)]NO_3 (**C3**)	90	107	15

Table 1. Size of nano coordination complexes by TEM and DLS

In the earlier work, we reported the synthesis, performance and application of **C3** complex, using Triton X-100, whereas in this work we report the synthesis of **C3** in presence of *cetyl*-trimethyl ammonium bromide (CTAB) which is a cationic surfactant and has changed the morphology and size of the nano coordination complex resulting in more positive and effective properties of the complex. Due to

change in the surfactant from neutral to cationic the morphology of the compound **C3** has shifted from rod to sphere.[35a] The dynamic light scattering experiments (Figure 2) provide a little different information about the size of the nano coordination complexes than that given by the TEM studies.

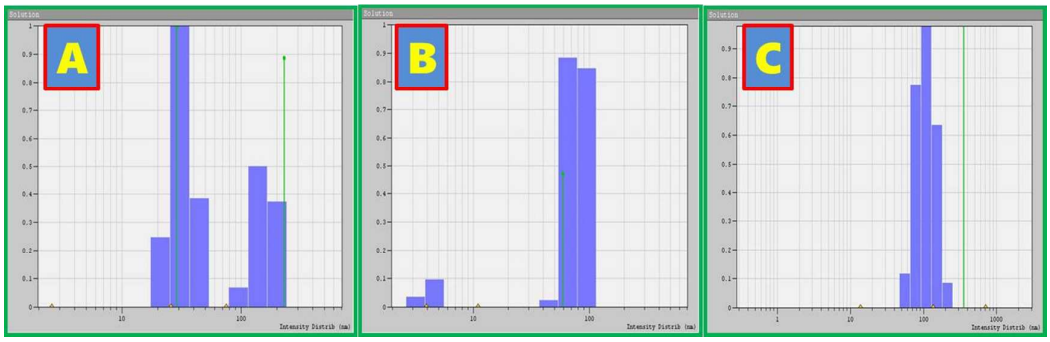

Figure 2. Size distribution plot for **C2** (A), **C1** (B) and **C3** (C) nano coordination complexes

Whereas the Number of Determinations/ cumulants: 3 and standard deviations of results ± 1-3 nm (**Table.1**). However, the hydration sphere was found to be smaller for the particles of SCN^- containing nano coordination complex than those of the other nano coordination complexes.

2.2 UV-visible spectroscopy

The electronic spectra of the nano coordination complexes were recorded in methanol and shows two strong bands in the UV region *i.e.* in the range of 273-284 nm assigned to the π-π* transition in benzimidazole group with extinction coefficients (log ε) ranging from 4.09-4.30. A broad and much less intense *d*–*d* band is observed in the region 650-750 nm indicating the presence of coordinated copper(II) ion with ligand L, while a shoulder at 300 nm is observed for the complexes due to ligand to metal charge transfer (LMCT).[36a,37]

2.3 Infrared spectroscopy

Infrared spectra of diamide ligand L : 3198 (υ_{NH} amide), 3034 (υ_{NH} benzimidazole), 1643 ($\upsilon_{C=O}$ amide-I), 1569 (υ_{C-N} amide-II), 1441 ($\upsilon_{C=N-C=C}$ benzimidazole), 742 ($\upsilon_{C=C}$ benzene). 1643, 1569 and 1441 cm^{-1} are assigned to amide-I (mainly $\upsilon_{C=O}$ amide stretch), amide-II (mainly υ_{C-N} amide stretch) and benzimidazole $\upsilon_{C=N-C=C}$ stretching frequencies, respectively. The benzene ring vibrations appear at 742 cm^{-1} (due to benzimidazole ring). The green coloured nano coordination complexes of copper(II)

shows an IR spectrum, wherein the amide-I shifts around 1620 cm^{-1}; while the amide-II and benzimidazole ($\upsilon_{C=N-C=C}$) bands shift around 1556 and 1450 cm^{-1}, respectively.

2.4 Electron paramagnetic resonance (EPR) spectroscopy

Figures S1-S3 (supplementary information) shows the EPR spectra of nano coordination complexes **C1**-**C3**. The value of $g_{\|}$ ranges from 2.27-2.32 and $g_{\perp}$ from 2.03-2.07 which is greater than 2.0023 (**table 2**).

Complex	$g_{\|}$	$g_{\perp}$	$A_{\|}$ (G)	α^2	$(g_{\|}/A_{\|})/10^{-4}$
[Cu(GBGA)Cl]Cl (**C1**)	2.27	2.05	156	0.56	145
[Cu(GBGA)(NO_3)]NO_3 (**C3**)	2.32	2.07	135	0.68	171
[Cu(GBGA)(SCN)]SCN (**C2**)	2.31	2.03	170	0.68	135

Table 2: X-Band EPR data of copper(II) nano coordination Complexes at 120K

2.5 Energy optimized structure

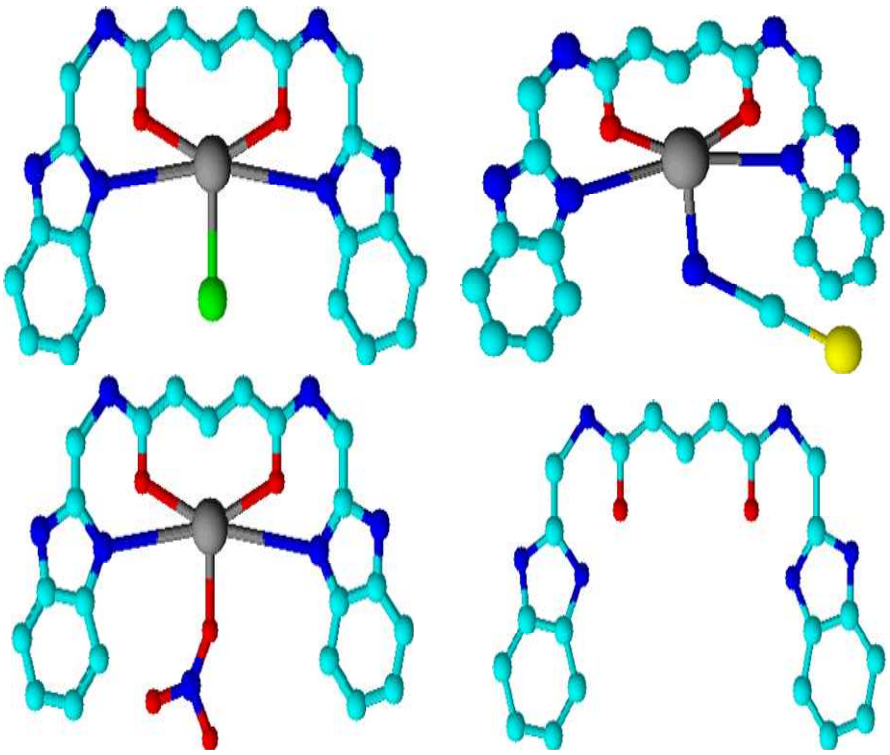

Figure 3. Energy optimized structures of monocationic copper(II) nano coordination complexes **C1** (*above left*), **C2** (*above right*), **C3** (*below left*) and ligand L (*below right*)

The energy optimization of **C1** was found to be 4745.5517 kcal/mol (figure 3). The H-bond of this operation is found to be 299.576 with stretch = 1236.581, angle =

1233.654, stretch bend = –6.917, dihedral = 231.136, improp torsion = 63.858, torsion stretch = –10.790, bend bend = –5.960, van der Waals = 2187.081, electrostatics = –97.915. The energy optimization of **C2** was found to be 805.8313 kcal/mol (figure 3) with stretch = 186.692, angle = 177.754, stretch bend = –0.404, dihedral = 174.896, improp torsion = 35.482, torsion stretch = –1.839, bend bend = –2.056, van der Waals = 165.035, electrostatics = 32.596, hydrogen bond = 405.861. The energy optimization of **C3** was found to be 6758.2864 kcal/mol (figure 3) with stretch = 1333.362, angle = 1050.934, stretch bend = –18.474, dihedral = 247.415, improp torsion = 29.944, torsion stretch = –12.656, bend bend = 9.063, van der Waals = 4065.143, electrostatics = –352.305, hydrogen bond = 37.676. The energy optimization of ligand L was found to be 5130.3028 kcal/mol (figure 3) with stretch = 865.318, angle = 1358.690, stretch bend = –0.094, dihedral = –0.014, improp torsion = 0.000, torsion stretch = –6.612, bend bend = 15.385, van der Waals = 2142.139, electrostatics = 12.940, hydrogen bond = 357.

2.6 Effect of copper (II) nano coordination complexes on nitric oxide synthesis

Lipopolysaccharide (LPS) (1 µg/ml) stimulated RAW 264.7 cells, to release substantial amounts of NO in 24 h incubation (0.3 µM). The inhibitory effect on LPS-induced NO production as shown by the compounds is shown in figure 4. The test compounds inhibited NO release, when added to the culture. **C1**, **C2** and **C3** reduced NO levels to 0.24, 2.1 and 2.5, µM respectively.

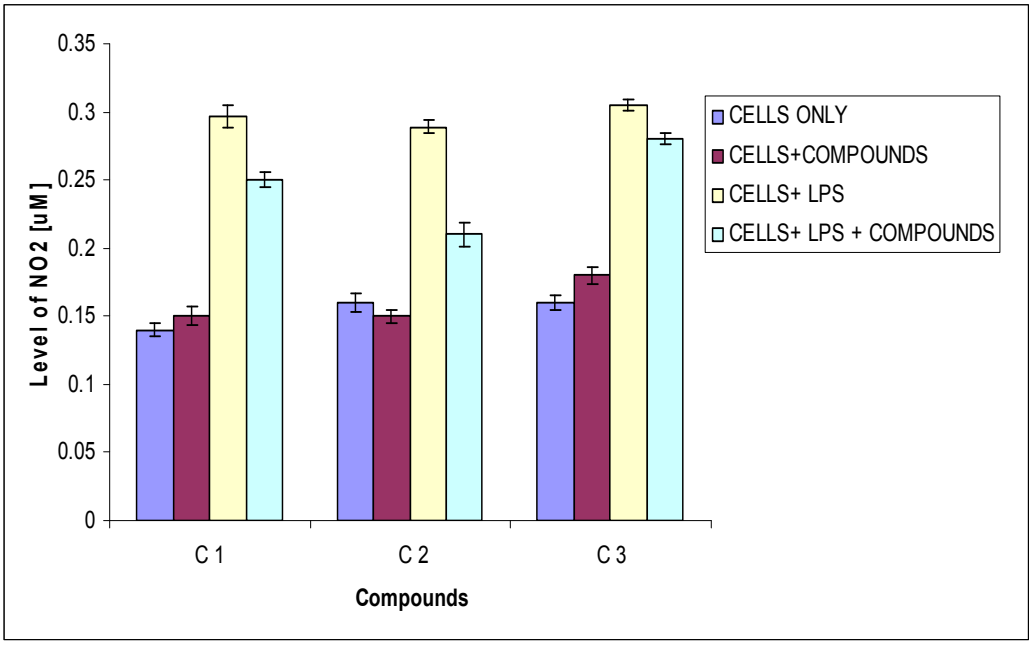

Figure 4. Effect of pretreatment with 100 μg/ml concentration of three different nano coordination complexes on nitric oxide production by LPS stimulated murine macrophage cell line RAW 264.7. After 24 hours of treatment, cell free supernatant from each well was taken and nitrite levels were measured. Values are expressed from six independent experiments performed in triplicate

2.7 Effect of copper (II) nano coordination complexes on super oxide production

24 hours administration of test compounds to RAW-264.7 cells, demonstrated a significant fall in LPS induced super oxide level (Figure 5). All the data points were plotted with respect to LPS induced super oxide level. The concentration of the produced super oxide in LPS treated cells was 0.25 µM. When test compounds were administered with LPS to the cells, these compounds demonstrated decreased super oxide level in terms of µM concentration.**C1** and **C3** reduced the LPS induced super oxide production from 0.235 and 0.232 µM to 0.215 and 0.200 µM, respectively, while **C2** showed significant reduction of super oxide level from 0.244 µM to 0.152µM.

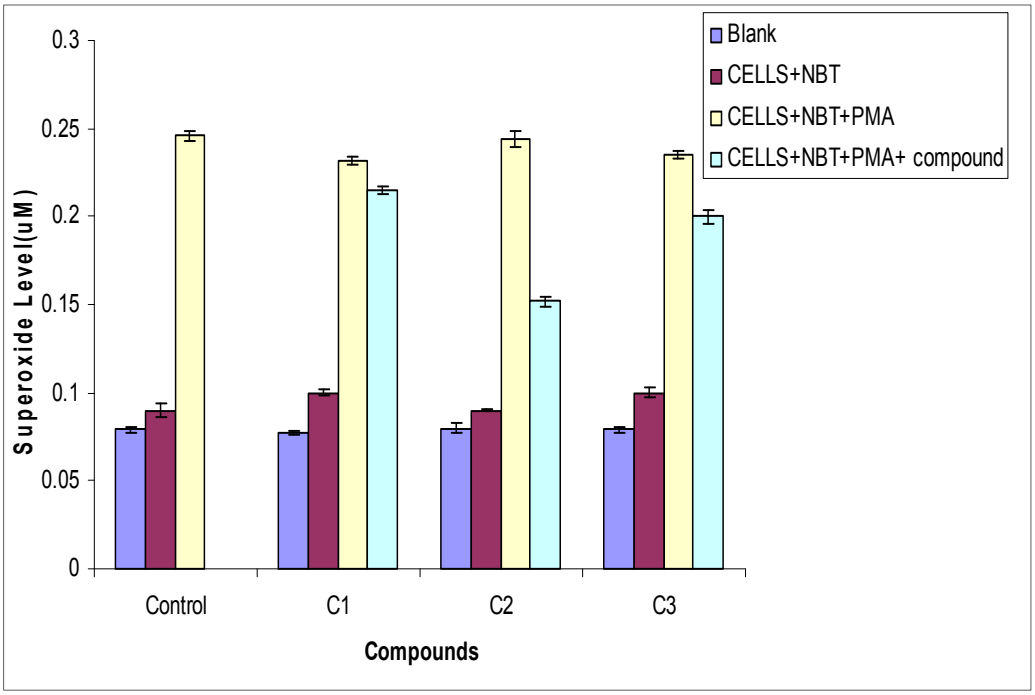

Figure 5. Effect of Copper(II) nano coordination complexes on superoxide production release in murine macrophage cell line RAW264.7. Cells were pretreated with LPS (1μg/ml) for inducing sufficient amount of superoxide in the culture medium and then treated with three different nano complexes of copper(II). After 24 hours of treatment superoxide level were measured. Values are expressed from six independent experiments performed in triplicate

2.8 Effect of copper (II) nano coordination complexes on cytotoxicity

The cytotoxicity of the test compounds were tested *in vitro* against normal cell lines (murine peritoneal macrophage cells) and human cancer cell lines Hela, MCF-7 and U-87. As shown in Figure 6 and 7, **C2** showed significant cytotoxicity towards Hela cell line at concentration of 100 µg/ml as compared to **C1** and **C3** under similar environment.

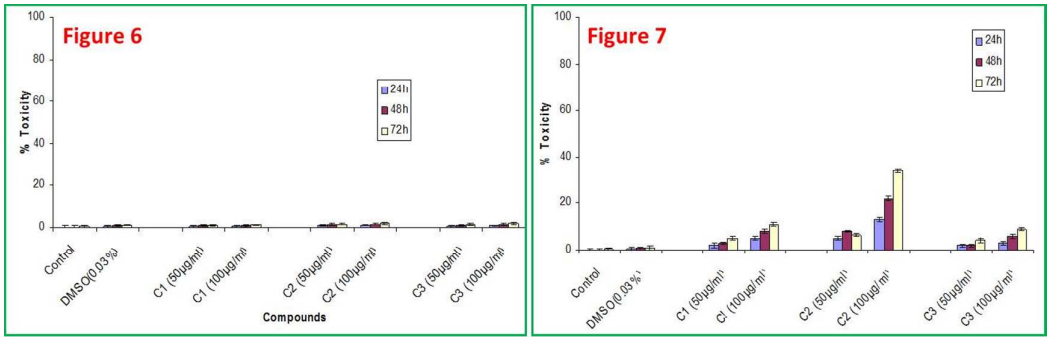

Figure 6. Effect of copper(II) nano coordination complexes on toxicity of normal cells. The *in vitro* cytotoxic effect against murine peritoneal macrophage cells was determined by MTT

assay. Cells were seeded on 96-well tissue culture plates and treated with two concentrations (50μg/ml and 100μg/ml) of three different nano complexes of copper(II) for different time periods (24 hrs., 48hrs. and 72 hrs.). Values are expressed from six independent experiments performed in triplicate and **Figure 7.** Effect of copper(II) nano coordination complexes on inhibition of cancer cell line. The *in vitro* anti-cancer effect against HeLa cell line was determined by MTT assay. Cells were seeded on 96-well tissue culture plates and treated with two concentrations (50μg/ml and 100μg/ml) of three different nano complexes of copper(II) for different time periods (24 hrs., 48hrs. and 72 hrs.). Values are expressed from six independent experiments performed in triplicate

Further analysis of **C2** for cytotoxicity showed that there was a significant enhancement in toxicity in both, dose and time dependent manner (Figures 8-10).

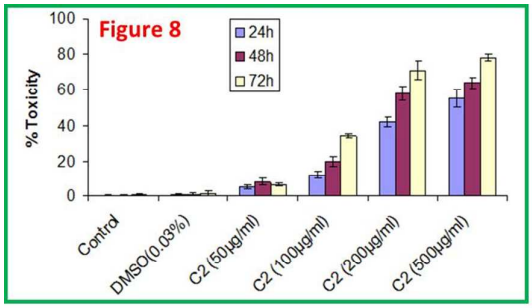

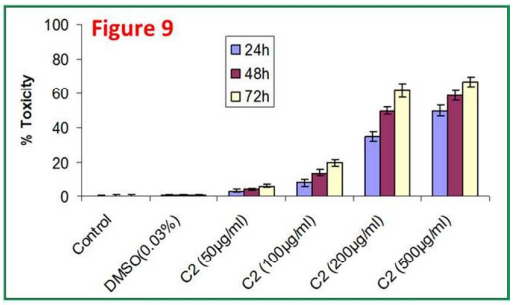

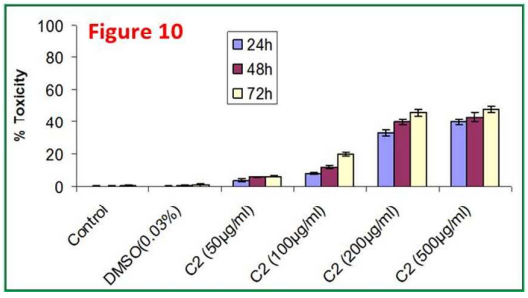

Figure 8. Effect of copper(II) nano coordination complex **C2** on inhibition of cancer cell line. The *in vitro* anti-cancer effect against HeLa cell line was determined by MTT assay. Cells were seeded on 96-well tissue culture plates and treated with four different concentrations (50μg/ml, 100μg/ml, 200μg/ml and 500μg/ml) of **C2** for different time periods (24 hrs. 48hrs. and 72 hrs.). Values are expressed from six independent experiments performed in triplicate, **Figure 9.** Effect of copper(II) nano coordination complex **C2** on inhibition of cancer cell line. The *in vitro* anti-cancer effect against breast cancer cell line MCF-7 was determined by MTT assay. Cells were seeded on 96-well tissue culture plates and treated with four different concentrations (50μg/ml, 100μg/ml, 200μg/ml and 500μg/ml) of **C2** for different time periods (24 hrs. 48hrs. and 72 hrs.). Values are expressed from six independent experiments performed in triplicate and **Figure 10.** Effect of copper(II) nano coordination complex **C2** on inhibition of cancer cell line. The *in vitro* anti-cancer effect against U-87 cell line was determined by MTT assay. Cells were seeded on 96-well tissue culture plates and treated with four different concentrations (50μg/ml, 100μg/ml, 200μg/ml and 500μg/ml) of **C2** for different time periods (24 hrs. 48hrs. and 72 hrs.). Values are expressed from six independent experiments performed in triplicate

HeLa, MCF-7 and U-87 cells exposed to different concentrations of **C2** ranging from 50 µg/ml to 500 µg/ml showed maximum toxicity at 500 µg/ml concentrations at 72 h interval. Whereas, there was no toxicity against normal cell lines (murine peritoneal macrophage cells).

2.9 Effect of test compounds on body weight of tumour transplanted mice

In the case of tumour control groups, the difference in body weight increased to around 11.5 g, whereas in the case of mice groups treated with test sample **C3**, the difference in body weight was around 4.7 g. In further studies, it decreased to 2.2 g and 0.6 g in the case of mice groups treated with **C1** and **C2** respectively. Figure 11a represents the pictographic representation of the treated mice whereas figure 11b is the graphical representation of the body weight of the treated mice.

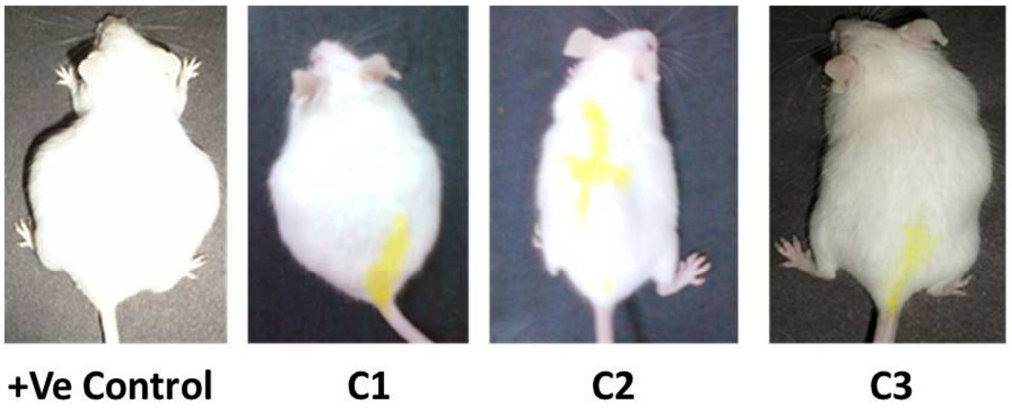

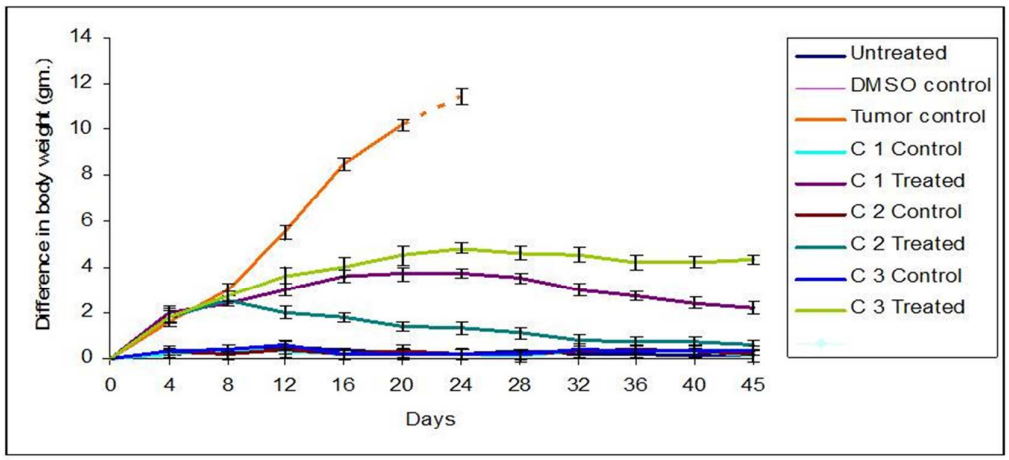

Figure 11a (*above*)**.** Pictographic representations of Balb/c mice showing the effect of copper(II) nano coordination complexes **C1**, **C2** and **C3** on the body weight of 7 days prior tumour transplanted mice and **Figure 11b** (*below*) Effect of copper(II) nano coordination complexes **C1**, **C2** and **C3** on the body weight of 7 days prior tumour transplanted mice. Treatment was given after 7 days of tumour transplantation in all the treated groups. **C1**

control, **C2** control and **C3** control groups received only test compounds **C1**, **C2** and **C3** respectively where as **C1** treated, **C2** treated and **C3** treated groups were tumour transplanted 7 days prior to treatment of test compounds **C1**, **C2** and **C3** respectively. After 30 days of treatment, graph was plotted on the basis of difference of body weight of treated groups with respect to tumour control groups.

2.10 Effect of test compounds on survival of tumour transplanted mice

In the tumour control group the mean survival time was 21 days, which increased to 100 days for mice treated with test **C3**, while it was found to extend even upto 120 days for mice treated with **C1**. In case of **C2** treatment, animals were found to be protected and survived even after 170 days with the gradual regression of tumour load (Figure. 12).

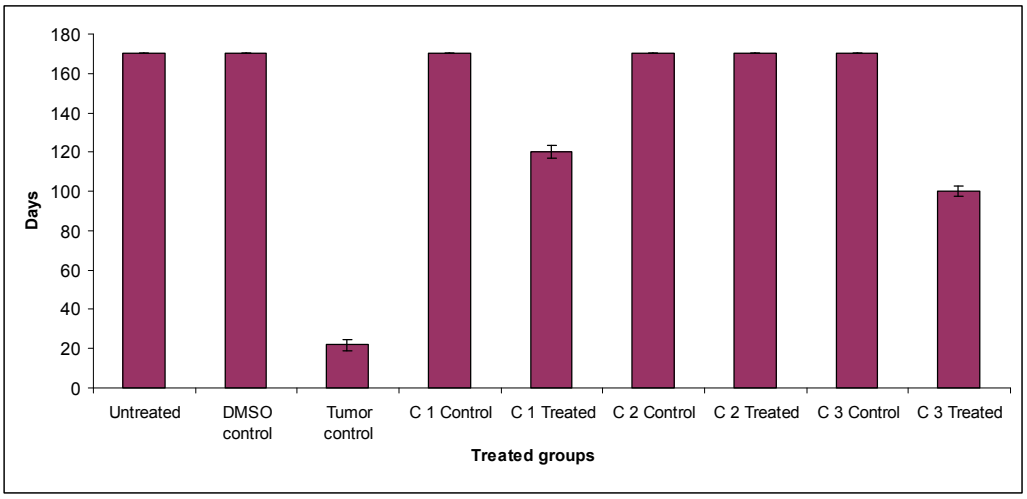

Figure 12 Effect of copper(II) nano coordination complexes **C1**, **C2** and **C3** on the survival of 7 days prior tumour transplanted mice. Treatment was given after 7 days of tumour transplantation in all the treated groups. **C1** control, **C2** control and **C3** control groups received only test compounds **C1**, **C2** and **C3** respectively where as **C1** treated, **C2** treated and **C3** treated groups were tumour transplanted 7 days

2.11 Murine peritoneal macrophage isolation

Previously established method has been used for peritoneal macrophage cell culture.[38] Balb/c mouse was sacrificed by cervical dislocation, sterilized with alcohol and was placed on dissecting tray which was earlier sterilized with alcohol and flamed. Mouse was stretched and pinned on the tray and outer layer of its skin was excised to expose under peritoneum and 5 ml of ice-cold incomplete medium (RPMI-1640) was injected in the animal by flame sterilized needle (22 G1). Point of injection was gently pressed with the finger for 10 seconds. Medium in the mouse body was checked for orange or

pinkish colour (while, if there is any contamination with body medium it turns whitish, and such contaminated animal's wasn't used). Little tapping of peritoneal cavity was done by hand, so that macrophages come out in suspension properly. Injected medium was then retrieved from peritoneal cavity by injection needle (18 G). 3-4 mL was usually retrieved from each animal. The cell suspension was centrifuged at 25 ^{o}C for 20 min. The erythrocytes in the cell pellets were lysed by hypotonic solution (0.2% NaCl). Isotonicity was restored with 1.6% NaCl solution. The cell suspension was centrifuged and the cells were washed twice and re-suspended in complete RPMI 1640 medium and cell number was adjusted to 1×10^6 cell/ml, which was determined by counting in a hemocytometer and cell viability was tested by the trypan-blue dye exclusion technique.

3. Discussion

TEM images reveal that the nano coordination complexes are spherical and each particle follows a symmetrical pattern. The above results are slightly different in agreement with dynamic light scattering experiments**,** giving a different range of size in liquid state. However, the hydration sphere of particles was found to be larger in comparison to that of TEM values. This may be due to solvent interaction (Water). Some of our complexes show extensive H-bonding interactions involving coordinated, lattice and solvent water molecules, nitrogen of the benzimidazole moiety, amide groups and co-anions,[35b] it could be the main reason to enhance the size of particles in liquid state. However, the hydration sphere was found to be smaller for the particles of SCN^{-} than those of other complexes. In electronic spectra, two peaks are observed in the range 272-284 nm, due to π–π^* transition in the –C=N–C=C– system of the benzimidazole group (these bands are slightly blue shifted with lowered extinction coefficient as compared to the ligand).[36] The *d-d* band is observed in the region 650-750 nm, while a shoulder at 300 nm is observed for the copper(II) nano coordination complexes due to LMCT.[37] In general these bands are assigned to the overlapping transition: $d_{yz,zx} \rightarrow d_{x2-y2}$ and $d_{xy} \rightarrow d_{x2-y2}$. The low energy of the *d-d* transition suggests severely distorted tetragonal copper (II) nano coordination complexes in the solution state. $CuCl_2$ salts in methanol show *d–d* bands (λ_{max}) at 900 nm. $CuCl_2$ also gives a *d–d* band (λ_{max}) at greater wavelength than **C1** indicates that free copper (II) ions is different from coordinated Cu(II) nano

coordination complexes. On the basis of the *d–d* spectra, we can say that there is no possibility for the production of free copper (II) ions from our nano coordination complexes in the solution phase. Henceforth, copper(II) metal capped by *bis*-benzimidazole group could provide suitable anchoring sites on the nano surface.

The free ligand shows characteristic single IR bands at 1643, 1569 and 1441 cm^{-1}. These are assigned to amide-I (mainly $\upsilon_{C=O}$ amide stretch), amide-II (mainly υ_{C-N} amide stretch) and benzimidazole $\upsilon_{C=N-C=C}$ stretching frequencies, respectively. The benzene ring vibrations appear at 742 cm^{-1} (due to benzimidazole ring). The ligand has a band at 3194 cm^{-1} which is assigned to stretching mode of υ_{N-H} benzimidazole, which are reported earlier.[35] The green coloured nano coordination complexes of copper(II) show an IR spectrum wherein the amide-I shifted at 1620 cm^{-1}; while the amide-II and benzimidazole ($\upsilon_{C=N-C=C}$) bands are shifted to 1556 and 1450 cm^{-1}, respectively for the compounds containing the co-anions nitrate and chloride, respectively. In all the cases the stretching frequency for the amide carbonyl is shifted by about 15-20 cm^{-1} with respect to the free ligand. This suggests that in the nano coordination complexes, the ligand is bound to copper(II) through the oxygen of amide carbonyl. This shifting in bands is indicative of copper(II) bound to the ligand in the nano coordination complexes.[36a,37a] The presence of nitrate and the thiocyanate anions in the respective complexes is justified by the presence of strong IR bands at 1384 cm^{-1} (υ_{O-N-O} sym str, ionic nitrate), nitrate ion is confirmed by a strong band in the region of 1340 to1385 cm^{-1} (bound monodentate nitrate) for the compounds and 2074 cm^{-1} (υ_{C-N} str.), which is resembled to N-coordinated υ_{C-N} stretching, 846 cm^{-1} (υ_{C-S} str.), respectively. Thus, the IR data clearly reveals that the copper ions are bound to the *bis*-benzimidazole ligand in the nano coordination complexes. X-Band EPR data of copper(II) nano coordination complexes typically indicate a d_{x2-y2} ground state ($g_{\|} > g_{\perp} > 2.0023$). Solution state spectra of the nano coordination complexes result less than four lines and broadening of $g_{\perp}$ line in some cases, thus indicating severe distorted tetragonal geometry. Broadening of $g_{\perp}$ reveals lowering in symmetry that manifest itself through rhombic splitting.

The $A_{\|}$ and $g_{\|}$ values for the complexes do not lie on the Peisach Blumberg Plots[37a] of $A_{\|}$ *vs* $g_{\|}$ for two nitrogen and two oxygen atoms in structural plane and suggests a distortion of the equatorial plane. The factor $g_{\|}/A_{\|}$ also indicates the distortion of coordination geometry. Higher the value of this factor, greater will be the distortion.

This is because when the geometry is no longer planar, the decreasing interaction of ground state d_{x2-y2} orbital with ligand orbitals resulted to lower the energy and thus repulsion between unpaired electron in d_{x2-y2} orbital and ligand electron decreases. As a result, this unpaired electron is now more delocalised and couples with the copper nucleus to a lesser extent. Here no nitrogen super hyperfine splitting could be observed, implying non-planarity of the complexes. $g_{\|}/A_{\|}$ follows the order SCN^{-}< Cl^{-}< NO_3^{-} indicating that distortion in coordination geometry is least for thiocyanate nano coordination complex. Thiocyanate nano coordination complex might be the one of reasons to exhibit significant inhibitory effect on NO syntheses and superoxide production and more power to kill the cancer cell line due to more planner and less distorted structure as compared to the other two nano coordination complexes.

The covalency factor α^2 has been calculated (**table 2**) by using the relationship[37] $g_{\|} = 2.0023 - 8\lambda\alpha^2/XY$. The '$\alpha^2$' depend on the nature of copper-ligand bond and decreases with increasing covalency of Cu–L bond. The minimum theoretical value of α^2 is 0.5 and maximum is 1.0.The α^2 of these nano coordination complexes ranges from 0.56-0.68 revealing very good amount of covalent character in Cu–L bond. It is very convincing to note that the chloro nano coordination complex in this series is relatively more covalent, while the nitrate and thiocyanate nano coordination complexes are more ionic.

The increasing order of covalency reflects the decreasing order of visible band energy *i.e.* greater covalency results in lowering of energy of orbital and henceforth the energy of $d_{xz,yz}/d_{xy} \rightarrow d_{x2-y2}$ transition is lowered. This is proved in the λ_{max} of the *d–d* band in the visible spectra data of these nano coordination complexes.

The present study reports the inhibitory effect of nano coordination complexes on the release of nitric oxide production, act as an antioxidant, *in vitro* cytotoxicity and anti-tumour activity. **C2** exhibited strong dose-dependent cytotoxic activity against the different cell lines due to potentially quantum dot range (5-10 nm) for co-anion thiocyanate. thiocyanate has back bonding[36b] ability and donates electrons from ligand to metal and *vice-versa*. Another structural aspect of these nano coordination complexes is that, they attain more surface area that enhanced more surface and bulk properties. Other two nano coordination complexes **C1** and **C3** also exhibited significant inhibitory effect on NO syntheses and superoxide production, but they were found to be lesser as compare to **C2**, due to higher nano size and effect of co-

anions, because the shape and size of a nano complex is important for how easily it can penetrate into a tumour.[37b] *Bis*-benzimidazole diamide ligand, which is coordinated by metallic salts also plays a vital role, acts as an antioxidant and an antitumour agent. The presence of imine nitrogen and carbonyl group, which might be functionalized by H-bonding network that further inhibits NO release. The presence of proton of NH amide, NH benzimidazole, CO amide may be attributed to a greater extent of H-bonding, which also contributed to inhibit the production of NO and superoxide. Recently, several reports have appeared in the literature describing the anti-cancer activity of copper(II) derivatives of several classes of nitrogen donors. They may have a mechanism of action which appears to be different from that of *cis*-platin. There are so many copper complexes, which show induced apoptosis in cultured mammalian cells[39,40] and are known to mediate significant cellular oxidative stress, promote membrane lipid peroxidation and interfere with mitochondria respiratory activity in fungal cells. Similarly **C1**, **C2**, and **C3** reported in the present work, show induced apoptosis in cultured cancer cell lines Hela, MCF-7 and U-87 and function to mediate cellular oxidative stress, promote membrane lipid peroxidation and cause to kill the cancer cell line. The *bis*-2-benzimidazoles have also received attention in past few years due to their anti-cancer activities. Recent developments on 2-substituted benzimidazoles have revealed varied heterocycles at 2-position to yield potent anticancer agents at various carcinoma cell lines. These include pyrimidine derivatives[41] pyrazoline derivatives[42] and thiazole derivatives.[43] *Bis*-benzimidazoles[44a] is another class of compounds exploited for discovery of anticancer agent. Hoechst-33342 [44b,45] and Hoechst-33258[46,47] are the openers of this series exhibiting *in vitro* antitumour as well as DNA topoisomerase I inhibitory activities. Huang *et al*. have synthesized benzimidazole isosteres which found as the most potent anticancer synthetic precursor of *bis*-benzimidazoles against human A-549, BFTC-905, RD, MES-SA, and HeLa carcinoma cell lines.[48] Benzimidazolyl-1,2,4-triazino[4,5-*a*]benzimidazol-1-one is another *bis*-benzimidazole analogue having significant activity against multidrug-resistant *P*-glycoprotein expressing cell lines.[49] Complexes of benzimidazoles as ligand with transition metal ions possess antitumour activity. Cu(II) complex of benzimidazolylmethyl-1,3-diaminopropane has the ability to intercalate into the double helix of DNA.[50] A Cu(II) complex of 2-pyridinylbenzimidazole-5-carboxylic acid has been found to exert potent topoisomerase II inhibitory activity.[51(a)] Thus, interest in the study of amide

complexes is derived from their ability to model active sites present in some metalloproteins and enzymes. The polypeptide chain surrounding the active site provides a suitable environment (hydrophilic). Imine nitrogen of benzimidazole and histidine has similar coordinating abilities (pK_a 5.5 and 6.0, respectively) which favors the pH control of metal ion coordination to imidazole nitrogen-atom, hence benzimidazole has been considered as a good mimic of histidine. Inducing agent LPS (1 μg/ml) was used to produce reactive oxygen, which is also being inhibited by protons of amide and benzimidazole of ligand moiety.

The energy optimized structure analysis of nano coordination complexes and ligand L reveals a significant interconnection in between stability of nano coordination complexes and inhibitory capability. The energy and number of hydrogen bonds of the optimized structure of **C2** was found to be 805.8313 kcal/mol and 405, which is quite different from ligand L. **C2** has lower optimized energy in comparison to **C1** and **C3** compounds, reemphasize more stability and more hydrogen-bonding network, that might tend to act as an anti tumour agent. The energy and number of hydrogen-bonds of optimized structures of **C1**, **C3** and ligand L are found to be 4745.5517 kcal/mol, 299; 6758.2864 kcal/mol, 37 and 5130.3028 kcal/mol, 357 respectively. These data are attributed to inter and intra connection of their stabilities, size of particles and their reactivity.

Various anticancer agents (also referred as antitumour, antiproliferative and antineoplastics) reported for treatment of varied kinds of cancers act through different mechanisms. However, the major side effect associated with these agents is cytotoxicity towards normal cells (murine macrophage cells) due to lack of selectivity for the abnormal cells. Therefore search on anticancer agent has been in continuum since many years. Benzimidazole being an isostere of purine based nucleic acid and an important scaffold in various biologically active molecules is widely explored for development of anticancer agents.[51(b)]

In the *in vivo* study, initially the mean survival time for tumour control group was 21 days. For the mice treated with test compound **C3**, **C1** and **C2**, the survival time extended to 100 days, 120 days and 170 days with the gradual regression of tumour load respectively. The *in vivo* results also show the impact of size and nature of co-anion, which were attributed to the function of benzimidazole moiety, size of nano

coordination complexes and roll of co-anion. These results confirmed that the shape and size of nano coordination complexes could influence their blood circulation in vivo toxicity[37b].

The inhibitory effect on LPS induced NO production was shown by all the compounds. Pre incubation of macrophage cells with different solids has effectively inhibited NO production in a concentration-dependent manner. This inhibition is not due to their cytotoxicity, as indicated by their cell viability values. The role of the free radical (NO) in inflammatory processes is well known.[52] Free radicals liberated from phagocyte cells are important in inflammatory processes because they are implicated in the activation of nuclear factor κB (NF-κB), which induces the transcription of inflammatory cytokines and COX-2. Furthermore, antioxidants have been shown to be able to effectively block the activation of NF-κB through the stabilization of NF-κB/IκB-α complex.[53] The results of this study showed that these compounds contain constituents that can inhibit the production of NO and superoxide.

4. Conclusion

A novel class of copper(II) nano coordination complexes **C1**, **C2** and **C3** functionalized by *bis*-benzimidazole diamide ligand, L have been synthesized and characterized by various spectroscopic methods. When added to the culture, these inhibited nitric oxide release and LPS induced super oxide production. These nano coordination complexes also showed significant *in vitro* cytotoxicity against human cervical cancer cell line Hela, breast cancer cell line MCF-7 and glioblastoma cell line U-87 at different concentrations, where as they are non-toxic against normal cells (murine peritoneal macrophage cells). *In vivo* study also reveals the same pattern of toxicity against tumour bearing mice. Body weight of tumour bearing mice decreased significantly in all the compounds tested with varying degrees. **C2** showed maximum reduction in body weight whereas **C3** showed the least, which is totally interconnected with the function of size and nature of co-anions of nano coordination complexes. Furthermore, survival of the treated mice potentiated the pattern of action, of nano coordination compounds as, the tumour bearing mice treated with **C2** survived around 150 days more as compared to tumour control group. It decreased to 100 and 80 days in the case of **C3** and **C1** treated groups, respectively. Overall, this study concludes that these nano coordination complexes could be used as a potent anti-cancer inhibitor or drug in the coming future.

5. Experimental Section

5.1. Materials and methods

Roswell Park Memorial Institute media (RPMI 1640) was purchased from Gibco TM, Griess reagent, aprotinin, leupeptin, phenylmethylsulfonylfluoride (PMSF), [*N*-(2-hydroxyethyl)piperazine-*N*′-(2-ethanesulfonic acid)] (HEPES), Dimethyl sulfoxide, $NaHCO_3$, *Escherichia coli* LPS, and all other required chemicals were purchased from Sigma (St. Louis, MO, USA). Fetal bovine serum (FBS) and trypsin–EDTA were purchased from Gibco-BRL (Gaithersburg, MD, USA). Ligand L was synthesized as earlier reported.[35a,37a]

In vitro studies were done in order to evaluate the nitric oxide inhibition, antioxidant and anti-cancer activity of the test compounds. This study used, *in vitro* model of mouse macrophage cell line RAW 264.7 cells, activated with LPS or PMA to induce nitric oxide and super oxide production. The inhibitory mechanism of nitric oxide production by the extract was limited to the measurement of nitrite concentration in micro molar concentrations. Inhibition of super oxide was assessed by NBT reduction assay. Swiss albino mice were used as a source of macrophages for *in vitro* studies. Inbred strain of pathogen free mice of either sex was used for various studies. Mice were maintained in the animal facility of Institute of Genomics and Integrative Biology, New Delhi, India. They were housed in polycarbonate cages and were provided tap water and animal diet. Animals were weighed, individually identified by tail mark and assigned into homogeneous weight groups. Animal room was maintained between 18-26 ^{o}C with light/dark cycles of 12 h intervals. *In vitro* studies were done in order to evaluate the immunomodulatory and anti-cancer activity of the test compounds. This study used *in vitro* model of mouse macrophage cell line RAW 264.7 cells activated with LPS or phorbol-12-myristate-13-acetate (PMA) to induce nitric oxide and super oxide production. The inhibitory mechanism of nitric oxide production by the extract was limited to the measurement of nitrite concentration in μM. Inhibition of super oxide was assessed by NBT reduction assay. The cells (RAW 264.7, MCF-7 and glioblastoma cell line U-87) were cultured and maintained in RPMI 1640 containing 2 mM glutamine, 10 mM HEPES, 1 mM sodium pyruvate adjusted to contain 1.5 g/L sodium bicarbonate, 10% heat-inactivated fetal bovine serum, 100 U/ml penicillin and 100 µg/ml streptomycin and 50 U/ml gentamycin.

Cells were grown at 37 ^{o}C with 5% CO_2 in humidifies air. The tumour (DL) cells were maintained *in vivo* in Swiss albino mice, by intraperitonial transplantation of 1 × 10^6 cells/mouse after every 7 days. Animal ethics committee of Department of Zoology, University of Delhi cleared the proposal and animals were handled according to the guidelines of Committee for Purpose of Control and Supervision of Experiments on Animals (CPCSEA), India.

5.2. Physical measurement

TEM studies were carried out using a Philips Morgagni 268 electron microscope operating at 80 kV at All India Institute of Medical Sciences (AIIMS), New Delhi, India. The TEM specimens were prepared by dispersing the powdered compounds in double distilled water and sonicating them. A drop of the sonicated solution was placed on to a porous carbon copper grid and then air dried. Perkin Elmer FTIR-2000 spectrometer used for comparable study of IR bands of the nano coordination complexes and the free ligand L by using KBr pellets at the Department of Chemistry, University of Delhi, Delhi, India. The light scattering experiments were performed on a Photocor FC, while, all the measurements were done at a scattering angle of 90° at temperature of 20 °C. Dilute solution of the samples were prepared by dispersing the powder in double distilled water followed by ultrasonic treatment for 15 min. Electronic spectra were obtained on a Shimadzu UV-Vis 1601 Spectrometer. Elemental analysis were obtained from University Science Instrumentation Centre (USIC), University of Delhi, Delhi, India. ^{1}H NMR spectra were recorded on a 300 MHz Bruker-spin instrument at Indian Institute of Technology (IIT), Delhi, India. X-Band EPR spectra of the copper(II) nano coordination complexes were recorded on a BRUKER-Spectrospin with a variable tempereature liquid nitrogen cryostat at 120K at IIT Kanpur, India in a frozen solution in methanol as solvent at liquid nitrogen temperature.

5.3 Synthesis of nano coordination complexes C3, C1 and C2

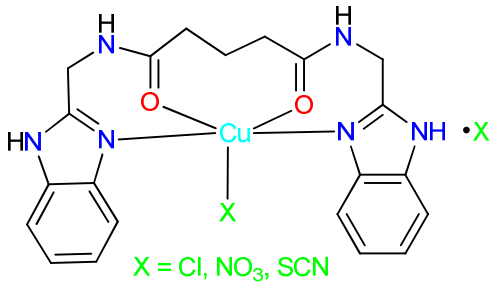

This method has been reported earlier.[35a,c] Micro emulsion I comprising of CTAB as the surfactant, *n*-butanol as the co-surfactant, *iso*-octane as the hydrocarbon phase, conductivity water and 0.227 mmol of ligand L were mixed together. Similarly, a micro emulsion II was prepared, containing the same constituents as micro emulsion I except that instead of the diamide ligand L, it had 0.227 mmol of $Cu(NO_3)_2.3H_2O$. The weight fractions of the various constituents in these micro emulsions were 16.66% of CTAB, 17.70% of *n*-butanol, 57.4% of *iso*-octane and 8.1% of the aqueous phase. The two micro emulsions were very slowly mixed together and stirred overnight on a magnetic stirrer results to the formation of green precipitates, which were separated by the nonpolar solvent and surfactant by centrifuging followed by washing with HPLC grade chloroform. The resultant compounds were then dried in vacuum and used without any further purification. Yield: 54% (160 mg). UV-Vis: λ_{max} (nm, log ε) in methanol: 276 (4.16), 283 (4.11), 710 (1.69). IR (KBr pellet, cm^{-1}): 3276 (υ_{NH} amide), 3061 (υ_{NH} benzimidazole), 1621 ($\upsilon_{C=O}$ amide-I), 1557 (υ_{C-N} amide-II), 1452 ($\upsilon_{C=N-C=C}$ benzimidazole), 738 ($\upsilon_{C=C}$ benzene), 1384 (υ_{O-N-O} sym stretch). Anal. Calc. for $Cu(C_{21}H_{22}N_6O_2)(NO_3)_2$: Cu, 10.91; C, 43.60; H, 3.87; N, 19.48; O, 21.09; Found: Cu, 10.80; C, 43.80; H, 3.71; N, 19.59; O, 21.22. Same procedure as discussed in section 5.3 has been used for the preparation of **C1** except that $CuCl_2.2H_2O$ was used in place of $Cu(NO_3)_2.3H_2O$. The green coloured precipitates were separated by adding the nonpolar solvent and surfactant by centrifuging followed by washing with HPLC grade chloroform. The resultant compound was then dried in vacuum and used without any further purification. Yield: 60% (155 mg). UV-Vis: λ_{max} (nm, log ε) in methanol: 272 (4.13), 284 (4.09), 695 (1.62). IR (cm^{-1}): 3241 (υ_{NH} amide), 3162 (υ_{NH} benzimidazole), 1621 ($\upsilon_{C=O}$ amide-I), 1552 (υ_{C-N} amide-II), 1455 ($\upsilon_{C=N-C=C}$ benzimidazole), 736 ($\upsilon_{C=C}$ benzene). Anal. Calc. for $Cu(C_{21}H_{22}N_6O_2)Cl_2$: Cu, 11.52; C, 51.33; H, 3.87; N, 15.23; Found: Cu, 11.39; C, 51.66; H, 3.72; N, 15.43. Before the

synthesis of **C2**, we synthesized $Cu(SCN)_2$ reagent by dissolving $CuCl_2.2H_2O$ in dry methanol (2 mL) and followed by the dropwise addition of. potassium thiocyanate solution in dry methanol. The precipitates of KCl were filtered off and the filtrate was used for the synthesis of **C2** as mentioned in procedure **C1**. Resultant green precipitate was separated by the nonpolar solvent and surfactant by centrifuging followed by washing with HPLC grade chloroform. The resultant compound was then dried in vacuum and used without any further purification. Yield: 55% (100 mg). UV-Vis: λ_{max} (nm, log ε) in methanol: 272 (4.35), 282 (4.30), 300 (3.80), 680 (1.68). IR (cm^{-1}): 3275 (υ_{NH} amide), 3141 (υ_{NH} benzimidazole), 1620 ($\upsilon_{C=O}$ amide-I), 1556 (υ_{C-N} amide-II), 1450 ($\upsilon_{C=N-C=C}$ benzimidazole), 739 ($\upsilon_{C=C}$ benzene), 2074 (υ_{C-N} str.), 846 (υ_{C-S} str.). Anal. Calc. for $Cu(C_{21}H_{22}N_6O_2)(SCN)_2$: Cu, 11.01; C, 48.27; H, 4.13; N, 19.48; O, 5.88; S, 11.02; Found: Cu, 11.23; C, 48.05; H, 4.31; N, 19.26; O, 6.07; S, 11.29.

5.5 Measurement of nitrite

Griess reagent[54] was used for the detection of nitrite concentration with minor modifications. Briefly, RAW 264.7 cells were plated at a density of 2×10^5 cells/well in a 96 well plate. Cells were incubated for 2 h and followed by addition of compounds. The final concentrations of the compounds in the cultures were 100 μg/ml. After 30 min incubation, RAW 264.7 cells were stimulated with 1 μg/ml LPS. The activated cells were further incubated for 24 h. Then, 100 μL supernatants were collected to determine nitrite concentration. Cell-free supernatant from each well was transferred to another 96-well flat-bottom plate and Greiss reagent (100 µL 1% sulphanilamide in 30% glacial acetic acid and 0.1% napthylethylenediamine dihydrochloride in 60% glacial acetic acid) was added. The absorbance of the samples was measured at 540 nM. Nitrite in samples was quantified by comparison with a standard curve. A nitrite multi point linear standard curve was determined using known concentrations of $NaNO_2$ ranging from 1.56 μM to 100 μM. Negative control cells (cells only) were grown under identical conditions, but were not exposed to the compound or LPS.

5.6 Nitro blue tetrazolium (NBT) reduction assay

The NBT reduction assay was carried out according to the previously described method[55] with minor modifications. Briefly, 100 μL (stock solution 100 μg/ml) of the test compounds were added to 2 × 10^5 RAW-264.7 cells. Inducing agent LPS (1 μg/ml) was used to produce reactive oxygen. Final volume was adjusted to 200 μL with RPMI in a flat bottom 96-well plate (Tarsons, India). The final concentrations of the compounds were 100 μg/ml per well. After incubation for 24 h at 37 ^{o}C in humidified 5% CO_2 incubator, medium was removed and washed once with warm PBS (37 ^{o}C). Fresh 100 μL of medium was added to each well with 5 μL of PMA (1 μg/ml) and 20 μL of NBT (1 mg/ml) except control. Plate was kept back to incubator for 2 h. After 2 h of incubation, the medium was removed and washed once with warm PBS (37 ^{o}C). Cells were fixed with 100% methanol for 1 min and after removing of methanol, 10 μL of 0.1% Triton X-100 was added along with 120 μL of 2M KOH and 140 μL of 100% DMSO. Cells were incubated for 5 min at room temperature on orbital shaker and absorbance were measured using ELISA micro plate reader at reference wavelengths of 620 nm.

5.7 Cytotoxicity assay

The cytotoxicity of compounds was investigated on cancer cell lines of different origin (HeLa, MCF-7 and U-87 cells). The cell lines were grown in RPMI supplemented with 10% (v/v) heat inactivated fetal bovine serum, 2 mM of glutamine, 100 U/ml of penicillin, and 100 μg/ml of streptomycin in a highly humidified atmosphere of 95% air with 5% CO_2 at 37 ^{o}C. Cell viability was assessed by the micro culture tetrazollium [3-(4,5-dimethylthiazol-2-yl)-2, 5-diphenyltetrazolium bromide (MTT) assay.[56] In brief, cells were seeded into a 96-well culture plate at 2 × 10^5 cells/well in a 100 μL culture medium. After incubation for 24 h, test compounds at two different concentrations were added to each well, respectively. The cells were incubated for another 24 h, 48 h and 72 h followed by the addition of 20 μL MTT solution (5 mg/ml) to each well and further cultivation for 4 h. The media with MTT were removed, and 100 μL of DMSO was added to dissolve formazan crystal at room temperature for 30 min. The absorbance of each cell was measured by UV-Vis spectrometer at 570 nm. The percentage of viable cells was calculated relative to untreated cells.

5.8 Viable/non-viable tumour cell count

The ascetic fluid was taken in a centrifuge tube and diluted 100 times. Then a drop of the diluted cell suspension was placed on the neubauer counting chamber and the number of cells in the 64 small squares was counted. The cells were then stained with trypan blue (0.4% in normal saline) dye. The cells that did not take up the dye were viable and those that took the stain were nonviable. These viable and nonviable cells were counted.

5.9 *In vivo* study

Six groups of Swiss albino mice were made each group having nine mice. Group I served as control in which mice were given no treatment. Group II as 0.3% DMSO control in which mice were injected with 0.3% DMSO intraperitonial. Animals of group III were tumour controls in which Dalton's Lymphoma (1×10^6 cells/mouse) were injected. Group IV, V and VI were treated with or without test nano coordination complexes **C1**, **C2** and **C3**, respectively. On day one body weight and girth size of each mice of all groups were measured. Dalton's Lymphoma cells were collected from the donor mouse and were suspended in sterile isotonic saline. The viable DL cells were counted (Trypan blue indicator) under the microscope and were adjusted at 1×10^6 cells/ml. 0.1 mL of Dalton's lymphoma cells per 10 g body weight of the animals was injected (i.p.) in group III, IV, V and VI. After seven days of tumour transplantation, mice of group IV, V and VI were treated with test compounds **C1**, **C2** and **C3** at the concentration of 3 mg/mice/day for 30 days.

5.10 Body weight

Body weights of the experimental mice were recorded both in the treated and control group at the beginning of the experiment (day 1) and sequentially on every 4^{th} day during the treatment period.

5.11 Survival of mice

The effect of test compounds **C1**, **C2** and **C3** on tumour transplanted mice was monitored by recording the mortality.

5.12 Energy optimized structure of copper(II) nano coordination complexes

To perform computational energy optimized structure of copper(II) nano coordination complexes and ligand L, were operated by Scigress 2.2.0 (Fujitsu) docking software. The minimized structures of these nano complexes were calculated by Mechanics Compute Engine 2.9.0.α1. Molecular Mechanics and reading parameters from molecular mechanics calculation will be carried out for all molecules. MM3 force field and Energy terms for the following interactions are included bond stretch, bond angle, dihedral angle, improper torsion, torsion stretch, bend bend, van der Waals, electrostatics, hydrogen bond. Conjugate gradient will be used to locate the energy minimum. All atoms will be moved at once during minimization. The dielectric value is 1.50. Van der Waals interactions between atoms separated by greater than 9.00 Å will be excluded. The van der Waals interactions list will be updated every 50 interactions. Optimization continues until the energy change is less than 0.00100000 kcal/mol, or until the molecule has been updated 300 times.

Acknowledgement

Author (Dr. S. C. Mohapatra) is thankful to Dr. D. S. Kothari UGC Post-doctoral fellowship (No.F.4-2/2006 (BSR)/13-215/2008(BSR) New Delhi for financial support. Authors are thankful to Prof. Pavan Mathur for helpful discussions and instrumental facilities and Dr. Gyantosh Jha, Principal, ARSD College, Delhi University.

Notes and references

1. S. J. Lippard, J. M. Berg, *Principles of Bioinorganic Chemistry*, University Science Books, Mill Valley, CA, 1994.
2. J. Reedijk, E. Bouwman, *Bioinorganic Catalysis*, 2nd ed., Dekker, New York, 1993.
3. K. D. Karlin, *Science*, 1993, **261**, 701–708.
4. D. E. Wilcox, *Chem. Rev*., 1996, **96**, 2435–2458.
5. B. Halliwell, J. M. C. Gutteridge, *Free radicals in biology and medicine*, 3rd ed., Oxford University Press, Oxford, UK, 1999.
6. R. M. Clancy, S. B. Abramson, *Proceed. Soc. Exp. Biol. Med*., 1995, **210**, 93–101.
7. J. R. Connor, P. T. Manning, S. L. Settle, W. M. Moore, G. M. Jerome, R. K. Webber, F. S. Tjoeng, M. G. Currie, *J. Pharmacol*., 1995, **273**, 15–24.

8. S. Tamir, S. R. Tannenbaum, *Biochimica. et. Biophysica. Acta*, 1996, **1288**, F31–F36.
9. M. G. Salgo, E. Bermudez, G. L. Squadrito, W. A. Pryor, *Arch. Biochem. Biophys*., 1995, **322**, 500–505.
10. M. G. Salgo, K. Stone, G. L. Squadrito, J. R. Battista, W. A. Pryor, *Biochem. Biophys. Res. Commun*., 1995, **210**, 1025–1030.
11. T. W. Yu, D. Anderson, *Mutat. Res*., 1997, **379**, 201–210.
12. Z. Guo, P. J. Sadler, *Adv. Inorg. Chem*. 2000, **49**, 183–306.
13. A. S. Mildvan, M. Cohn, *J. Biol. Chem*., 1966, **241**, 1178–1193.
14. E. Bouwman, W. L. Driessen, J. J. Reedijk, *Coord. Chem. Rev*., 1990, **104**, 143–172.
15. S. O. Podunavac-Kuznonovic, V. M. leovac, N. U. Perisic-Janjic, J. Ragon, L. Balaz, *J. Serb. Chem. Soc*., 1999, **64**, 381–388.
16. S. A. Galal, K. H. Hegab, A. M. Hashem, N. S. Youssef, *Eur. J. Med. Chem*., 2010, **45**, 5685–5691
17. M. Devereux, D. O'Shea, M. O'Connor, H. Grehan, G. Connor, M. McCann, G. Rosair, F. Lyng, A. Kellett, M. Walsh, D. Egan, B. Thati, *Polyhedron*, 2007, **26**, 4073–4084.
18. D. A. Horton, G. T. Bourne, M. L. Smythe, *Chem. Rev*., 2003,**103**, 893–930.
19. H. Kucukbay, R. Durmaz, E. Orhan, S. Gunal, *II Farmaco*, 2003, **58**, 431–437.
20. V. Klimesova, J. Koci, K. Waisser, J. Kaustova, *II Farmaco*, 2002, **57**, 259–265.
21. Y. He, B. Wu, J. Yang, D. Robinson, L. Risen, R. Ranken, L. Blyn, S. Sheng, E. E. Swayze, *Bioorg. Med. Chem. Lett*., 2003,**13**, 3253–3256.
22. G. Ayhan-Kilcigil, N. Altanlar, *II Farmaco*, 2003, 58, 1345–1350.
23. N. S. Pawar, D. S. Dalal, S. R. Shimpi, P. P. Mahulikar, *Eur. J. Pharm. Sci*., 2004, **21**, 115–118.
24. N. Bharti, M. T. Shailendra, G. Garza, D. E. Cruz-Vega, J. Castrogarza, K. Saleem, F. Naqvi, M. R. Maurya, A. Azam, *Biorg. Med. Chem. Lett*., 2002, **12**, 869–871.
25. S. Zden, D. Atabey, S. Yildiz, H. Goker, *Bioorg. Med. Chem*., 2005, **13**, 1587–1597.
26. G. N. V´azquez, R. Cedillo, A. Hernandez-Campos, J. Yepez, F. H. Luis, J. Valldez, R. Morales, R. Cortes, M. Hernandez, R. Castillo, *Bioorg. Med. Chem. Lett*., 2001, **11**, 187–190.

27. A. A. Spasov, I. N. Yozhitsa, L. I. Bugavea, V. A. Anisimova, *Pharm. Chem. J*., 1999, **33**, 232–243.
28. T. A. Kabanos, A. D. Keramidas, D. Mentzafos, U. Russo, A. Terzis, J. M. Tsangaris, *J. Chem. Soc. Dalton Trans*., 1992, 2729–2734.
29. S. A. Wank, *Am. J. Physiol*., 1998, **274**, 607–613.
30. P. J. Iship, M. D. Closier, M. C. Neville, L. M. Werbel, D. B. Capps, *J. Med. Chem*., 1972, **15**, 951–954.
31. M. Gokce, S. Utku, S. Gur, A. Ozkul, F. Gumus, *Eur. J. Med. Chem*., 2005, **40**, 135–141.
32. E. Sizova, S. Miroshnikov, V. Polyakova, N. Gluschenko, A. Skalny, *J. Biomaterials and Nanotech*, 2012, **3**, 97–104.
33. T. A. Baytukalov, N. N. Glushchenko, O. A. Bogoslovskaya, I. P. Olkhovskaya, G. E. Folmanis, I. P. Arsentieva, *RF Patent No*. 2296571, 2007.
34. T. A. Baytukalov, N. N. Glushchenko, O. A. Bogoslovskaya, I. P. Olkhovskaya, I. O. Leipunsky, A. N. Zhigach, E. A. Shafranovsky, *RF Patent No*. 2306141, 2007.
35. (a) S. C. Mohapatra, H. K. Tiwari, M. Singla , B. Rathi, A. Sharma, K. Mahiya, M. Kumar, S. Sinha, S. S. Chauhan, *J. Biol. Inorg. Chem*., 2010, **15,** 373–385. (b). S. C. Mohapatra, M. S. Hundal, P. Mathur, *Spectro Chimica Acta: Part A*, 2011,**79,** 1634-1641. (c) M. Singla, S. C. Mohapatra , S. Ahmad, *Mat. Chem. and Phy.,* 2012, **137**, 118-128.
36. (a) M. Gupta, P. Mathur, R. J. Butcher, *Inorg. Chem*., 2001, **40**, 878–888. (b) R. J. Allenbaugh, A. L. Rheingold, L. H. Doerrer, *Dalton Trans*., 2009, 1155-1163.
37. (a) S. C. Mohapatra, P. Mathur, *Spectrochim. Acta A*, 2011, **78**, 612–616. (b).Y. Wang, K. C. L. Black, H. Luehmann, W. Li, Y. Zhang, X. Cai, D. Wan, S. Y. Liu, M Li, P Kim, Z-Y Li, L V. Wang, Y. Liu, Y. Xia, *ACS Nano*, 2013, **7(3)**, 2068–2077.
38. P. Parajuli, S. M. Singh, A. Kumar, A. Sodhi, *The Cancer J*., 1997, **10**, 222–228.
39. F. Saczewski, E. Dziemidowicz-Borys, P. J. Bednarski, R. Grunert, M. Gdaniec, P. Tabin, *J. Inorg. Biochem*., 2006, **100**, 1389–1398.
40. B. Rosenberg, *Metal Ions Biol. Syst*., 1980, **11**, 127–196.
41. H. T. Abdel-Mohsen, F. A. Ragab, M. M. Ramla, H. I. El Diwani, *Eur. J. Med. Chem*., 2010, **45**, 2336–2344.

42. M. Shaharyar, M. M. Abdullah, M. A. Bakht, J. Majeed, *Eur. J. Med. Chem*., 2010, **45**, 114–119.

43. (a) Y. Luo, F. Xiao, S. Qian, W. Lu, B. Yang, *Eur. J. Med. Chem*., 2011, **46**, 417–422. (b) M. Devereux, D. O. Shea, A. Kellett, M. McCann, M. Walsh, D. Egan, C. Deegan, K. Kedziora, G. Rosair, H. Muller-Bunz, *J. Inorg. Biochem*., 2007, **101**, 881–892.

44. (a) L. A. R. Solano, I. Aguiniga, M. L. Ortiz, R. Tiburcio, A. Luviano, I. Gegla, E. Santiago-Osorio, V. M. Ugalde-Saldivar, R. A. Toscano, I. Castillo, *Eur. J. Inorg. Chem*., 2011, 3454–3460. (b) A. Chen, C. Yu, B. Gatto, L. F. Liu, *Proc. Natl. Acad. Sci. U.S.A*., 1993, **90**, 8131–8135.

45. A. Y. Chen, C. Yu, A. L. Bodley, L. F. Peng, L. F. Liu, *Cancer Res*., 1993, **53**, 1332–1337.

46. E. H. Kraut, T. Fleming, M. Segal, J. A. Neidhart, B. C. Behrens, J. MacDonald, *Invest. New Drugs*, 1991, **9**, 95–96.

47. B. Tolner, J. A. Hartly, D. Hochhauser, *Mol. Pharamcol*., 2001, **59**, 699.

48. S. T. Huang, I. J. Hseib, C. Chena, *Bioorg. Med. Chem*., 2006, **14**, 6106–6119.

49. J. Styskala, L. Styskalova, J. Slouka, M. Hajduch, *Eur. J. Med. Chem*., 2008, **43**, 449–455.

50. Q. Zhou, P. Yang, *Inorg. Chim. Acta*, 2006, **359**, 1200-1206.

51. (a) S. A. Galal, K. H. Hegab, A. M. Hashem, N. S. Youssef, *Eur. J. Med. Chem*., 2010, **45**, 5685–5691; (b) Y. Bansal, O. Silakari, *Bioorg. and Med. Chem*., 2012, **20**, 6208–6236.

52. G. R. Schinella, H. A. Tournier, J. M. Prieto, P. M. de-Buschiazzo, J. L. Rios, *Life Sci*., 2002, **70**, 1023–1033.

53. Y. C. Huang, J. H. Guh, Z. J. Cheng, Y. L. Chang, T. L. Hwang, C. N. Lin, C. M. Teng, *Life Sci*., 2001, **68**, 2435–2447.

54. Y. S. Chi, B. S. Cheon, H. P. Kim, *Biochem. Pharmacol*., 2001, **61**, 1195–1203.

55. E. Pick, J. Charon, D. Mizel, *J. Reticuloendothel. Soc*., 1981, **30**, 581–593.

56. M. C. Alley, D. A. Scudiero, A. Monks, M. L. Hursey, M. J. Czerwinski, D. J. Fine, B. J. Abbott, J. G. Mayo, R. H. Shoemaker, M. R. Boyd, *Cancer Res*., 1988, **48**, 589–601.